Danmarks Tekniske Universitet

46755 Renewables in Electricity Markets

Assignment 1

Christian Witt, s203667
Frederik Skou Fertin, s203679
Jacob Sterup Skaarup, s203693
Thomas Reenberg Trosborg, s203658

2024-03-24

Contents

1 Step 1: Copper-plate, single hour **1**

1. a) Justification of market-clearing price using KKT 2

2 Step 2: Copper-plate, multiple hours **3**

3 Step 3: Optimization vs equilibrium **5**

4 Step 4: Network constraints **6**

4. a) Nodal setup 6

4. b) Zonal setup 8

5 Step 5: Balancing market **11**

6 Step 6: Reserve market **12**

References **15**

A Appendix **16**

A. a) Market-clearing optimization model - KKT conditions 16

A. b) Nodal daily prices 17

A. c) Contribution table 17

Nomenclature

$\delta_{k,\tau}$ Change in wind power production for windfarm *k*, at time τ

η_b (Dis)charging efficiency of battery *b* [%]

λ Dual variable of balance constraint

μ, σ, τ Dual variables

$\overline{P}_b^B$ Maximum (dis)charging rate of battery *b* [MW]

$\overline{P}_{dt}^D$ Demand of load *d* in hour *t* [MWh]

$\overline{P}_g^G$ Max power generation of generator *g* [MW]

$\overline{P}_{wt}^W$ Forecasted Wind Power production of wind farm *w* in hour *t* [MWh]

$\overline{P}_g^R, \underline{P}_g^R$ Up- and down ramping limit of generator *g* [MW]

θ Voltage angle

ATC Available transfer capacity between zones [MW]

B_{nm} Susceptance of the line connecting bus n to m [p.u.]

C_g^d Down reserve bid price for generator *g* [$/MW]

C_g^u Up reserve bid price for generator *g* [$/MW]

c_g^G Offer price of generator *g* [$/MWh]

$D^{\downarrow}$ Up reserve demand [%]

$D^{\uparrow}$ Up reserve demand [%]

F_{nm} Capacity of line running from bus n to m [MW]

P_i^H Daily demand of hydrogen for electrolyzer *i* [tonnes]

$r_{i,t}^{\downarrow}$ Down reserve for a generator at time t [MW]

$r_{i,t}^{\uparrow}$ Up reserve for a generator at time t [MW]

SOC_{bt} State of Charge of battery *b* in hour *t* [MWh]

SOC_b^{init} Initial State of Charge of battery *b* [MWh]

$u_d t^D$ Bid price of demand *d* in hour *t* [$/MWh]

LMP Locational Marginal Price [$/MWh]

Choice of electric power network

The goal of this report is to model and clear the market in an electrical system as seen from the system perspective. For this a case study is used and here the updated IEEE RTS 24-Bus System is chosen [1].

1 Step 1: Copper-plate, single hour

Given the set of conventional generators, $\mathcal{G}$, the set of wind farms, $\mathcal{W}$, and the set of demands, $\mathcal{D}$, the market-clearing optimization model is constructed:

$$\max_{\boldsymbol{p^D}, \boldsymbol{p^G}, \boldsymbol{p^W}} \sum_{i \in \mathcal{D}} u_i^D \, \boldsymbol{p_i^D} - \sum_{j \in \mathcal{G}} c_j^G \, \boldsymbol{p_j^G} \tag{1}$$

$s.t.$

$$0 \leq \boldsymbol{p_i^D} \leq \overline{P}_i^D \; : \; \underline{\boldsymbol{\mu}}_{\boldsymbol{i}}, \overline{\boldsymbol{\mu}}_{\boldsymbol{i}} \qquad \forall i \in \mathcal{D} \tag{2}$$

$$0 \leq \boldsymbol{p_i^G} \leq \overline{P}_i^G \; : \; \underline{\boldsymbol{\sigma}}_{\boldsymbol{i}}, \overline{\boldsymbol{\sigma}}_{\boldsymbol{i}} \qquad \forall i \in \mathcal{G} \tag{3}$$

$$0 \leq \boldsymbol{p_i^W} \leq \overline{P}_i^W \; : \; \underline{\boldsymbol{\tau}}_{\boldsymbol{i}}, \overline{\boldsymbol{\tau}}_{\boldsymbol{i}} \qquad \forall i \in \mathcal{W} \tag{4}$$

$$\sum_{i \in \mathcal{D}} \boldsymbol{p_i^D} - \sum_{j \in \mathcal{G}} \boldsymbol{p_j^G} - \sum_{k \in \mathcal{W}} \boldsymbol{p_k^W} = 0 \; : \; \boldsymbol{\lambda} \tag{5}$$

This market-clearing optimization model maximizes social welfare by subtracting the cost of power generation from the utility of the demand. The cost of wind power generation is assumed to be 0 \$/MWh and thus not included in the objective function. The model variables consist of $\boldsymbol{p_i^G}$, the power generated by generator i, $\boldsymbol{p_i^D}$, the power consumed by load i, and $\boldsymbol{p_i^W}$, the power produced by wind farm i. They are all non-negative and capped by: for $\mathcal{G}$ the maximum generation capacity, for $\mathcal{D}$ the bid volume of electricity, and for $\mathcal{W}$ the offered power from each wind farm. Finally, the model includes the power balance equation, which ensures that the power consumption and production are balanced. The dual of the balance constraint, λ, is the market clearing price.

Running the above market-clearing algorithm for the first hour of the chosen case we compute the market clearing price, λ, and the social welfare of the solution. The market-clearing price is 10.52 \$/MWh, and the social welfare is \$44,597.

Furthermore, the profit of each generator and wind farm, and the utility of each demand can be calculated based on the optimal solution. Of the 12 conventional generators in the network only generator 7-10 are active where generator 7 is the marginal generator. As it is the marginal generator, generator 7 does not turn a profit as it is selling at its offered cost. Generator 7's offered cost is 10.52 \$/MWh, which as expected corresponds to the identified market-clearing price. The 6 wind farms are all active as they have the lowest cost of the system and the demand exceeds their capacities. The utilities of each consumer are shown in table 1. Likewise, the bids and profit of the active generators are shown in table 2. It is observed that despite the higher cost of the conventional generators, their additional capacity results in higher profits than for the wind turbines, with the exception of generator 7 which is the marginal generator.

Table 1: Utility for each consumer in the system.

Demand	1	2	3	4	5	6	7	8	9
Utility [$]	775	693	1,284	1,361	1,309	2,513	2,303	3,141	160
Demand	10	11	12	13	14	15	16	17	–
Utility [$]	1,386	4,869	3,560	292	92	2,385	3,351	2,356	–

Table 2: Offer price, dispatched generation, and profit for each active generator. G_7 is the marginal generator and therefore has no profit.

Generator	W_1	W_2	W_3	W_4	W_5	W_6	G_7	G_8	G_9	G_{10}
Offer [$/MWh]	0	0	0	0	0	0	10.52	6.02	5.47	0
Dispatched [MWh]	99.83	84.42	71.29	115.32	74.43	105.15	125.40	400	400	300
Profit [$]	1,050	888	750	1,213	783	1,106	0	1,800	2,020	3,156

1. a) Justification of market-clearing price using KKT

The KKT conditions can be derived for the full market-clearing optimization model, see appendix A. a). However, to justify the market-clearing price, λ we only need to look at the optimization model for the marginal generator, G7, which sets the price. The optimization which the marginal generator is bidding based on can be written as a minimization problem.

$$\min_{\boldsymbol{p_7^G}} \boldsymbol{p_7^G}(c_7^G - \lambda) \tag{6}$$

$$s.t.$$

$$0 \leq \boldsymbol{p_7^G} \leq \overline{P}_7^G \ : \ \underline{\boldsymbol{\sigma}}_{\boldsymbol{7}}, \overline{\boldsymbol{\sigma}}_{\boldsymbol{7}} \tag{7}$$

The Lagrangian relaxation is:

$$\mathcal{L}\left(p_7^G, \underline{\sigma}_7, \overline{\sigma}_7\right) = p_7^G(c_7^G - \lambda - \underline{\sigma}_7 + \overline{\sigma}_7) - \overline{\sigma}_7 \overline{P}_7^G \tag{8}$$

The corresponding KKT conditions are:

$$\frac{\partial \mathcal{L}}{\partial p_7^G} = c_7^G - \lambda - \underline{\sigma}_7 + \overline{\sigma}_7 = 0 \tag{9}$$

$$0 \leq p_7^G \qquad \perp \quad \underline{\sigma}_7 \geq 0 \tag{10}$$

$$0 \leq \overline{P}_7^G - p_7^G \qquad \perp \quad \overline{\sigma}_7 \geq 0 \tag{11}$$

As stated in table 2, $P_7^G = 125.4MW,\ c_7^G = 10.52\$/MWh$, and the market-clearing price is $\lambda = 10.52\$/MWh$. The maximal generation capacity for generator G7 is 155 MW. By inspecting the results from solving the market-clearing optimization model, the dual variables of the constraints on the generation capacity of generator G7 can be found. For the hour in question $\overline{\sigma}_7 = 0$ and $\underline{\sigma}_7 = 0$. By inspection of the KKT conditions when using the specified values, it is shown that the KKT conditions are fulfilled for the marginal generator in our optimal solution from the market-clearing problem. This shows that the derived market-clearing price ensures that the market is in a Nash equilibrium, where no market participator can benefit by deviating from the current solution.

2 Step 2: Copper-plate, multiple hours

The previous model can be expanded to include a time index and additional actors can be added, as well as inter-temporal constraints. We define the set of hours in one day, $\mathcal{T}$, and the set of batteries, $\mathcal{B}$. The following model includes ramping constraints on the conventional generators, the addition of batteries, and electrolyzers with a minimum daily hydrogen production on each of the wind farms.

$$\max_{\boldsymbol{p^D},\boldsymbol{p^G},\boldsymbol{p^{ch}},\boldsymbol{p^{dis}},\boldsymbol{SOC},\boldsymbol{p^H}} \sum_{t\in\mathcal{T}} \left[\sum_{i\in\mathcal{D}} u_{it}^{D}\, \boldsymbol{p_{it}^{D}} - \sum_{j\in\mathcal{G}} c_{j}^{G}\, \boldsymbol{p_{jt}^{G}} \right] \tag{12}$$

$s.t.$

$$0 \le \boldsymbol{p_{it}^{D}} \le \overline{P}_{i}^{D}, \qquad \forall i \in \mathcal{D},\, \forall t \in \mathcal{T} \tag{13}$$

$$0 \le \boldsymbol{p_{it}^{G}} \le \overline{P}_{i}^{G}, \qquad \forall i \in \mathcal{G},\, \forall t \in \mathcal{T} \tag{14}$$

$$0 \le \boldsymbol{p_{it}^{W}} \le \overline{P}_{it}^{W}, \qquad \forall i \in \mathcal{W},\, \forall t \in \mathcal{T} \tag{15}$$

$$\sum_{i\in\mathcal{D}} \boldsymbol{p_{it}^{D}} - \sum_{j\in\mathcal{G}} \boldsymbol{p_{jt}^{G}} - \sum_{k\in\mathcal{W}} \left(\boldsymbol{p_{kt}^{W}} - \boldsymbol{p_{kt}^{H}}\right) + \sum_{l\in\mathcal{B}} \left(\boldsymbol{p_{lt}^{ch}} - \boldsymbol{p_{lt}^{dis}}\right) = 0 \;:\; \boldsymbol{\lambda_t} \qquad \forall t \in \mathcal{T} \tag{16}$$

$$\underline{P}_{i}^{R} \le \boldsymbol{p_{i(t)}^{G}} - \boldsymbol{p_{i(t-1)}^{G}} \le \overline{P}_{i}^{R}, \qquad \forall i \in \mathcal{G}, \forall t \in \mathcal{T} \tag{17}$$

$$\underline{P}_{i}^{R} \le \boldsymbol{p_{i0}^{G}} \le \overline{P}_{i}^{R}, \qquad \forall i \in \mathcal{G} \tag{18}$$

$$\boldsymbol{SOC_{it}} = \boldsymbol{SOC_{i(t-1)}} + \eta_i \boldsymbol{p_{it}^{ch}} - \frac{1}{\eta_i} \boldsymbol{p_{it}^{dis}}, \qquad \forall i \in \mathcal{B}, \forall t \in \mathcal{T}_{+} \tag{19}$$

$$\boldsymbol{SOC_{i1}} = SOC_{i}^{init} + \eta_i \boldsymbol{p_{i1}^{ch}} - \frac{1}{\eta_i} \boldsymbol{p_{i1}^{dis}}, \qquad \forall i \in \mathcal{B} \tag{20}$$

$$\boldsymbol{SOC_{i(24)}} \ge SOC_{i}^{init} \qquad \forall i \in \mathcal{B} \tag{21}$$

$$0 \le \boldsymbol{p_{it}^{ch}}, \boldsymbol{p_{it}^{dis}} \le \overline{P}_{i}^{B} \qquad \forall i \in \mathcal{B}, t \in \mathcal{T} \tag{22}$$

$$0 \le \boldsymbol{SOC_{it}} \le \overline{SOC}_i \qquad \forall i \in \mathcal{B}, t \in \mathcal{T} \tag{23}$$

$$0 \le \boldsymbol{p_{it}^{H}} \le \frac{1}{2} \overline{P}_{i}^{W,nom}, \qquad \forall i \in \mathcal{W},\, \forall t \in \mathcal{T} \tag{24}$$

$$\boldsymbol{p_{it}^{H}} \le \overline{P}_{it}^{W}, \qquad \forall i \in \mathcal{W},\, \forall t \in \mathcal{T} \tag{25}$$

$$\sum_{t\in\mathcal{T}} \boldsymbol{p_{it}^{H}} \ge P_{i}^{H}, \qquad \forall i \in \mathcal{W} \tag{26}$$

Clearing the market for 24 hours without inter-temporal constraints leads to the prices in table 3. When the inter-temporal constraints are added the prices increase as seen in table 4. This is due to the electrolyzers taking up parts of the cheap wind turbine production and theoretically also the ramping constraints making the generators less flexible (in the inter-temporal market clearing the ramping constraints are never active). At the same time the battery is performing price arbitrage thereby increasing demand during cheap hours and increasing supply during expensive hours to profit on the price difference. Notably, the battery is modelled with a (dis)charging efficiency of 99% to enable it since it was observed that the battery was never trading in the market with an efficiency of 95%.

Table 3: Market price of electricity over 24 hours without inter-temporal constraints.

Hour	1	2	3	4	5	6	7	8	9	10	11	12
Price [$/MWh]	10.52	6.02	6.02	6.02	6.02	6.02	10.52	10.52	10.89	10.89	10.89	10.89
Hour	13	14	15	16	17	18	19	20	21	22	23	24
Price [$/MWh]	10.89	10.89	10.52	10.52	10.89	10.89	10.89	10.52	10.52	10.52	10.52	6.02

Table 4: Market price of electricity over 24 hours with inter-temporal constraints.

Hour	1	2	3	4	5	6	7	8	9	10	11	12
Price [$/MWh]	10.52	10.52	10.52	10.52	10.52	10.52	10.52	10.52	10.52	10.89	10.89	10.89
Hour	13	14	15	16	17	18	19	20	21	22	23	24
Price [$/MWh]	10.89	10.89	10.67	10.67	10.89	10.89	10.89	10.52	10.52	10.52	10.52	10.52

The market clearing with inter-temporal constraints results in hour 15 and 16 having the same spot price, which is not equal to the generation cost of the marginal generator. If the battery had not participated in the market clearing the price in hour 15 and 16 would have been 10.52$/MWh. The battery is charging in these hours to benefit from the price dip, but it is willing to pay 10.67$/MWh and not only 10.52, which is the offer price of the marginal generator. This number comes from the fact that the battery can sell energy later at a price of 10.89$/MWh - incorporating the double converter losses ($10.89 \cdot 0.99^2 = 10.67$) results in the price the battery is willing to charge at. The market price is changed since the battery uses the rest of the available capacity of the marginal generator and then creates a vertical crossing in the supply and demand curve with the next cheapest generator, which has an offer price of 10.89$/MWh. The dual variable becomes 10.67$/MWh as this is the price the battery would be willing to trade at if any additional capacity was available.

During the hour from 08:00 to 09:00 the bid price of demand D13 drops to 10.2 $/MWh and for D16 to 7.0 $/MWh. Figure 1 shows the different merit order curves for the market clearing for the two hours from 07:00 to 09:00. The supply curve is unchanged, while the demand curve changes with the aforementioned bids. The spot price of the two hours is unchanged, but the demand of D13 and D16 is no longer supplied in the market as their bids are lower than the cost of the marginal generator. In table 4 this also results in the spot price lowering for hour 9 when introducing intertemporal constraints/behaviour, whereas the price is non-decreasing when introducing intertemporality in all other hours.

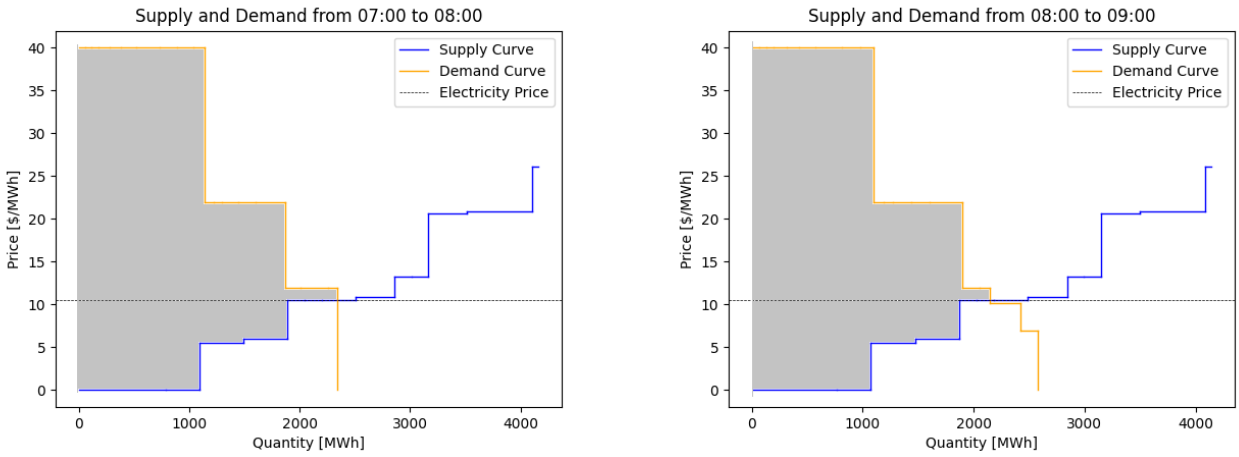

Figure 1: Merit order curves for 7-8 and 8-9 showing how the price is set and can differ between two hours.

The social welfare derived from running the copperplate market clearing model with and without the different intertemporal components can be seen in table 5. As mentioned earlier, the ramping constraints are not strong enough to change the market clearing equilibrium. However, it can be observed that the battery increases the social welfare of the system by shifting the supply and demand curves in select hours. The extra consumption of the electrolyzers reduces the computed social welfare of the system by effectively removing available wind power from the system as the electrolyzers are not included as a load with a bid price.

Table 5: Computed social welfare for demands and generators for 24 hours.

Added components	None	Ramping	Battery	H_2	Combined
Social Welfare [$]	1,290,958	1,290,958	1,293,007	1,265,771	1,265,835
Index	100	100	100.16	98.05	98.05

3 Step 3: Optimization vs equilibrium

When determining the equilibrium, the optimization problem is divided into individual optimization problems for each agent in the market, as well as the price setter problem. An equilibrium model will still optimize for every single agent, e.g. minimize the cost of a generator or maximize utility for the demand. In the expanded problem, the batteries and electrolyzers now also acts as agents in the market and are optimized. Each agent is optimized over time, resulting in a summation over all time steps in the objective function and a set of constraints for all time steps. Deriving the KKTs for each agent and collecting them yields the mixed complementarity problem. Below is an example of the Lagrangian function for a single generator with inter-temporal constraints, i.e. the ramping constraints. Here μ_t is the dual variables for the ramping constraints and σ_t the dual variable for the generator capacity constraint.

$$\begin{aligned}\mathcal{L}\left(p_t^G, \underline{\mu}, \overline{\mu}, \underline{\sigma}, \overline{\sigma}\right) = &- \sum_{t\in\mathcal{T}} \left(c_t^G - \lambda_t\right) \boldsymbol{p_t^G} \\ &+ \sum_{t\in\mathcal{T}} \underline{\mu}_t \cdot \left(\underline{P}_t^R - \boldsymbol{p_t^G} + \boldsymbol{p_{(t-1)}^G}\right) + \sum_{t\in\mathcal{T}} \overline{\mu}_t \cdot \left(\boldsymbol{p_t^G} - \boldsymbol{p_{(t-1)}^G} - \overline{P}_t^R\right) \\ &+ \sum_{t\in\mathcal{T}} \underline{\sigma_t} \cdot \left(-p_t^G\right) + \sum_{t\in\mathcal{T}} \overline{\sigma}_t \cdot \left(p_t^G - \overline{P}_t^G\right)\end{aligned} \tag{27}$$

The KKT's can be determined as the partial derivatives of the Lagrangian function, the inequality constraints, and the complementarity conditions as no equality constraints are present in the generator problem. It is assumed that the system runs in a cyclic mode and during the first hour of a day $t-1$ therefore refers to the last hour of the previous day, and the other way around for the last hour of a day and $t+1$. In eq. (28) dual variables with both index t and $t+1$ appears due to the presence of primal variables with index t and $t-1$ in eq. (27). A given primal variable p_t^G will therefore be multiplied with both $\underline{\mu}_t$ and $\underline{\mu}_{t+1}$ when the sum is written out.

$$\frac{\partial \mathcal{L}}{\partial p_t^G} = c_t^G - \lambda_t - \underline{\mu}_t + \underline{\mu}_{t+1} + \overline{\mu}_t - \overline{\mu}_{t+1} - \underline{\sigma_t} + \overline{\sigma_t} = 0, \qquad \forall t \in \mathcal{T} \tag{28}$$

$$0 \leq p_t^G, \qquad \perp \underline{\sigma}_t \geq 0, \quad \forall t \in \mathcal{T} \tag{29}$$

$$0 \leq \bar{P}^G - p_t^G, \qquad \perp \bar{\sigma}_t \geq 0, \quad \forall t \in \mathcal{T} \tag{30}$$

$$0 \leq p_t^G - p_{t-1}^G - \underline{P}^R, \qquad \perp \underline{\mu}_t \geq 0, \quad \forall t \in \mathcal{T} \tag{31}$$

$$0 \leq \bar{P}^R + p_{t-1}^G - p_t^G, \qquad \perp \bar{\mu}_t \geq 0, \quad \forall t \in \mathcal{T} \tag{32}$$

The KKT's for the optimization problem would be the same for this agent as all generators act under the same conditions. These equations would then not be for just one generator, but for all the generators $i \in \mathcal{G}$. This will eventually be the same for the equilibrium model when constructing the complementarity problem. The addition of an inter-temporal constraint will not make the optimization model and equilibrium model dissimilar. Only external influence, such as a market cap, will influence the similarity of the two market clearing models. Using this approach on the electrolyser or battery would yield the same result but is omitted for brevity.

4 Step 4: Network constraints

4. a) Nodal setup

The model is now extended to take the network constraints into account. In a nodal setup, a balance equation is included for each node $n \in \mathcal{N}$, where $\mathcal{N} = \{N_1, N_2, ..N_k\}$. Furthermore, in these balance equations the power flow between node n and all connected nodes $m \in \mathcal{N}_n$ is included (see constraint (34)). In the nodal setup, all cable capacities are modeled and respected with the addition of constraint (35). The reason for the negative lower bound, is that the power can flow in both directions. Finally, constraint (36) sets the initial voltage angle at node $n = 0$ to $\theta_{N_1} = 0$ to set a reference. As only voltage angle differences are included in the problem, setting this reference limits the number of optimal solutions from infinite to one.

$$\max_{\boldsymbol{p^D}, \boldsymbol{p^G}, \boldsymbol{p^{ch}}, \boldsymbol{p^{dis}}, \boldsymbol{SOC}, \boldsymbol{p^H}, \boldsymbol{\theta}} \sum_{t\in\mathcal{T}} \left[\sum_{i\in\mathcal{D}} u_{it}^D \, \boldsymbol{p_{it}^D} - \sum_{j\in\mathcal{G}} c_{jt}^G \, \boldsymbol{p_{jt}^G}\right] \tag{33}$$

$s.t.$

eqs. $(13) - (26)$

$$\sum_{i \in \mathcal{D}_n} \boldsymbol{p_{it}^D} - \sum_{j \in \mathcal{G}_n} \boldsymbol{p_{jt}^G} - \sum_{k \in \mathcal{W}_n} (\boldsymbol{p_{kt}^W} - \boldsymbol{p_{kt}^H}) + \sum_{l \in \mathcal{B}_n} \left(\boldsymbol{p_{lt}^{ch}} - \boldsymbol{p_{lt}^{dis}} \right) + \sum_{m \in \mathcal{N}_n} B_{nm}(\boldsymbol{\theta_{nt}} - \boldsymbol{\theta_{mt}}) = 0 \ : \ \boldsymbol{\lambda_{nt}} \qquad \forall n \in \mathcal{N}, \forall t \in \mathcal{T} \qquad (34)$$

$$-F_{nm} \leq B_{nm}(\boldsymbol{\theta_{nt}} - \boldsymbol{\theta_{mt}}) \leq F_{nm} \qquad \forall m \in \mathcal{N}_n, \forall n \in \mathcal{N}, \forall t \in \mathcal{T} \qquad (35)$$

$$\boldsymbol{\theta_{N_1\, t}} = 0 \qquad \forall t \in \mathcal{T} \qquad (36)$$

In this problem formulation, the power flow from node n to node m is modeled with the DC power flow equation $f_{nm} = B_{nm}(\boldsymbol{\theta_{nt}} - \boldsymbol{\theta_{mt}})$, where B is the susceptance matrix and θ_{nt} is the voltage angle of node n at time t. Naturally, this is a simplification of the true AC power flow. As the AC power flow equations are non-linear and non-convex, this is a necessary simplification to ensure that the optimal solution is found. However, the simplification is based on a list of assumptions; (i) cable resistances are disregarded, (ii) all voltages are 1 p.u., (iii) voltage angle differences are sufficiently small, and (iv) reactive power flows are disregarded. These assumptions are serious and should be taken into account when evaluating the results.

The dual variables obtained from eq. (34) equal the nodal marginal prices of electricity. Figure 2 shows the resulting LMPs of 2 select hours of the cleared day - the first and ninth hour, which correspond to the generally lowest and highest nodal prices in the network, respectively. From this it can be observed how the prices are generally lower at the top of the network, where a large number of generation units are located, than the bottom of the network, where a lot of the demand is located. The network visualizations of the two hours also highlight three transmission lines in red. The three lines are congested during all hours of the day, where the amount of power transmitted from the area excess supply is limited. This creates the significant price difference, where the upper nodes are at around 6$/MWh and the lower nodes are around 11$/MWh during hour 1 and 14 $/MWh during hour 9.

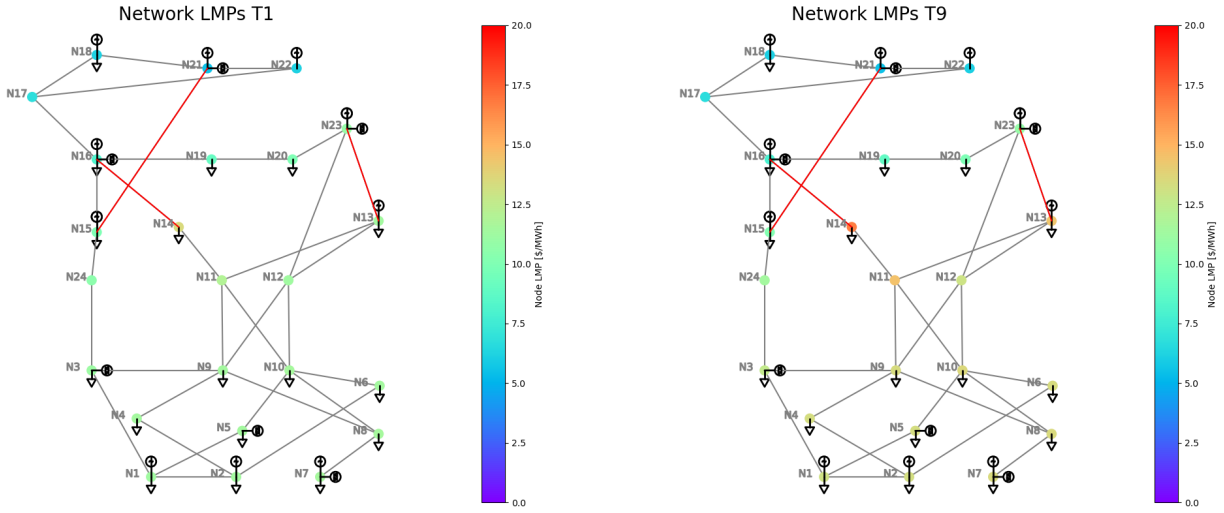

Figure 2: Locational marginal prices (LMPs) for the nodal setup during hours 1 and 9 (i.e., the hour with the lowest and highest prices, respectively). The red lines indicate congested lines.

The congested lines create a significant price differential between the two nodes connected at each end of the

line - however price differences are observed between all nodes in the network when just one line is congested. Highlighting the line connecting node 14 and node 16 which is congested, a large price difference with $\lambda_{N_{14}t_9} = 16.71$ \$/MWh and $\lambda_{N_{16}t_9} = 7.82$ \$/MWh is observed. The price $\lambda_{N_{11}t_9} = 14.48$ \$/MWh, which is also directly connected to node 14 also has a different price than $\lambda_{N_{14}t_9}$, but not as significantly as seen on the two ends of the congested line.

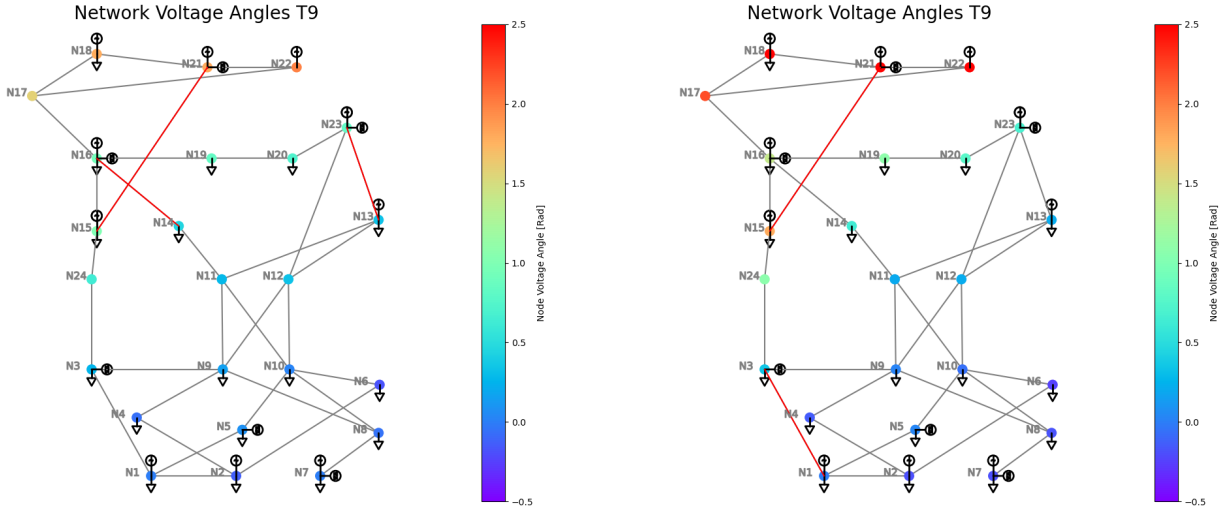

(a) Line capacity of line 23 (line from node 14 to node 16): 250 MW **(b)** Line capacity of line 23 (line from node 14 to node 16): 500 MW

Figure 3: Nodal voltage angles (with $V_{ref} = 0$ at node 1) for the nodal setup during the hour T19 (i.e., the hour with the highest prices).

When running the nodal market clearing it was observed that three lines were always congested. As an additional sensitivity analysis the capacity of the line between node 14 and 16 is increased from 250 MW to 500 MW - we continue to look at hour 9. Looking at fig. 3 the nodal voltage angles along with the congested lines are depicted. General notes on the nodal voltage angles would be that the high voltage angles are in the supply excess area and drops down through the network. The line upgrade succeeds in removing the congestion on the line $N_{14} - N_{16}$ and also $N_{13} - N_{23}$, but creates a new congestion on line $N_1 - N_3$. The upgraded line allows the upper area nodes to increase their voltage level further with extra generation. The LMPs of node 14 and node 16 are now $\lambda_{N_{14}t_9} = 10.30$ \$/MWh and $\lambda_{N_{16}t_9} = 10.03$ - the price gap has been reduced significantly. The average nodal price has also been reduced from 11.44 \$/MWh to 10.03 \$/MWh with the grid upgrade and the social welfare increased from \$1,229,906 to \$1,241,131, which indicates an increase in social welfare of over \$10,000 per day by upgrading the one line.

4. b) Zonal setup

A zonal model is now introduced where the grid is divided into the three zones as shown in fig. 4.

Now, rather than including a power balance equation for each node, one is included for each zone $z \in \mathcal{Z}$. Furthermore, instead of modelling each cable with a line limit constraint, now only interconnectors between zones are modelled (900 MW between zone 1 and 2 and 2000 MW between zone 2 and 3).

For the zonal setup, the two aforementioned constraints for balancing the nodes and comply with the capacities for the transmission lines are now changed. This is seen in equations 38 and 39. It is also seen that the variables

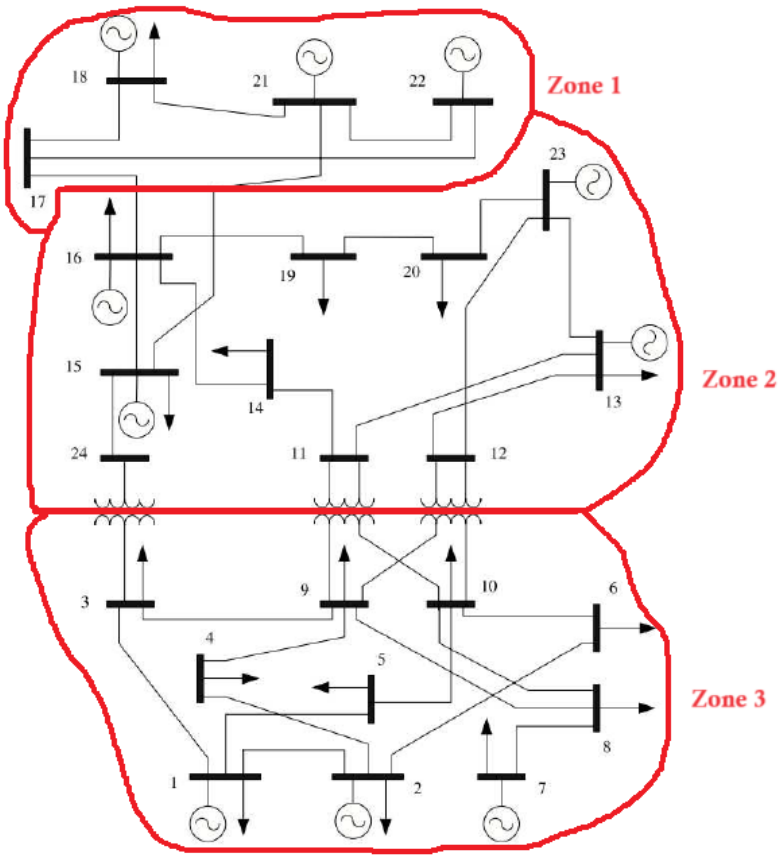

Figure 4: Division of network into 3 zones.

are changed, so the voltage angle θ is not a variable, but f is, which is the power trade between zones.

$$\max_{\boldsymbol{p^D},\boldsymbol{p^G},\boldsymbol{p^{ch}},\boldsymbol{p^{dis}},\boldsymbol{SOC},\boldsymbol{p^H},\boldsymbol{f}} \sum_{t\in\mathcal{T}} \left[\sum_{i\in\mathcal{D}} u_{it}^{D}\, \boldsymbol{p_{it}^{D}} - \sum_{j\in\mathcal{G}} c_{jt}^{G}\, \boldsymbol{p_{jt}^{G}} \right] \tag{37}$$

$s.t.$

eqs. $(13) - (26)$

$$\sum_{i\in\mathcal{D}_a} \boldsymbol{p_{it}^{D}} - \sum_{j\in\mathcal{G}_a} \boldsymbol{p_{jt}^{G}} - \sum_{k\in\mathcal{W}_a} \left(\boldsymbol{p_{kt}^{W}} - \boldsymbol{p_{kt}^{H}}\right) + \sum_{l\in\mathcal{B}_a} \left(\boldsymbol{p_{lt}^{ch}} - \boldsymbol{p_{lt}^{dis}}\right) + \sum_{b\in\mathcal{Z}_a} \boldsymbol{f_{ab}} = 0 \;:\; \boldsymbol{\lambda_{at}} \qquad \forall a \in \mathcal{Z}, \forall t \in \mathcal{T} \tag{38}$$

$$-ATC_{ab} \leq \boldsymbol{f_{ab}} \leq ATC_{ab} \qquad \forall b \in \mathcal{Z}_a,\ \forall a \in \mathcal{Z},\ \forall t \in \mathcal{T} \tag{39}$$

Using the same data as in previous models and setting the ATC to be the sum of capacity of the interconnecting cables. Solving the optimization problem yields the zonal prices of fig. 5. Here the prices in zone 2 and 3 are identical throughout the day, indicating that there is no congestion on the connecting lines. Zone 1 has a low and flat price throughout the day indicating a congestion on the lines connecting zone 1 and 2, as zone 1 and 3 are not connected. The low price in zone 1 can be explained by the presence of wind farm 5 with a bid of 0 \$/MWh and generator 8 to 10 which are the cheapest in the system with a maximum bid of 6.02\$/MWh. At the same time there is only a single demand in zone 1 constituting just 11% of the total system demand. The system can be compared

to how the German electrical grid is today and the implications of dividing Germany into multiple price zones.

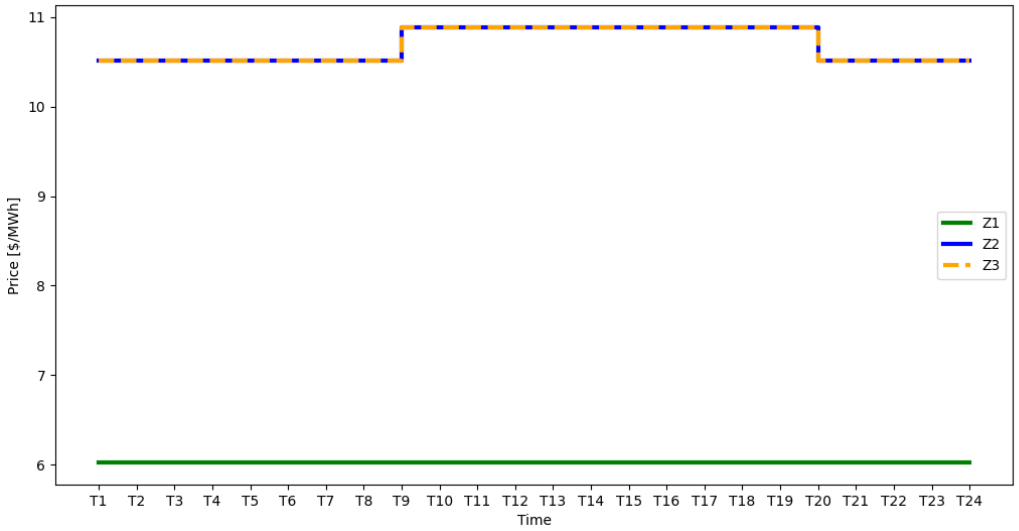

Figure 5: Price in the three zones for each hour of the day.

The sensitivity of the zonal prices to changes in the ATC between the zones can be examined. In fig. 6 two scenarios are tested where the ATC between zone 1 and 2, and zone 2 and 3 is adjusted until the prices deviate from fig. 5. In fig. 6a a small increase of 11% of the ATC between zone 1 and 2 will lead to uniform prices from the morning to the evening, and only result in congestion during the night. This connection is therefore slightly underdimensioned. In order to see congestion and different prices between zone 2 and 3 the ATC must be more than halved to 850 MW. This is seen as a price difference during peak hours in fig. 6b.

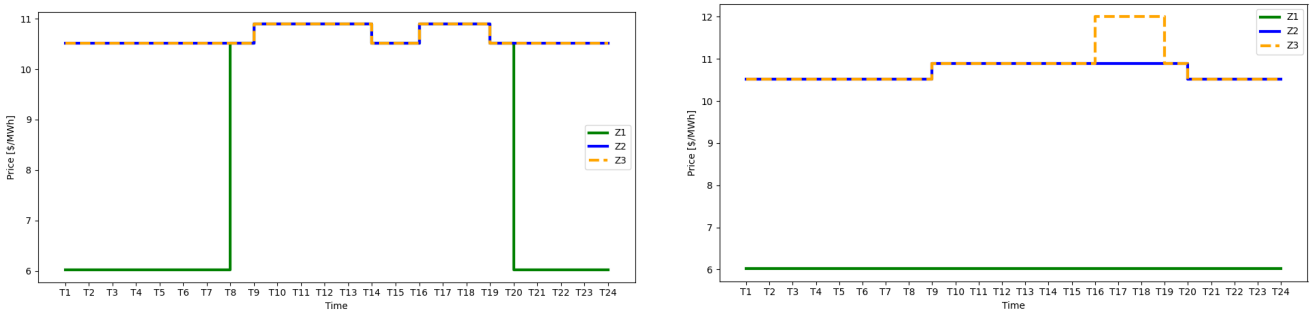

(a) ATC between zone 1 and 2 increased from 900 MW to 950 MW. **(b)** ATC between zone 2 and 3 reduced from 2000 MW to 850 MW.

Figure 6: Sensitivity of zonal prices as ATC between zones are changed.

4. b).1 Nodal vs. Zonal setup

Comparing the base cases of the nodal and zonal market clearing, the implications of the different setups for market participants can be examined. The key metrics used to compare the two frameworks are social welfare generated and generation unit profits. However, there are some general takeaways from the earlier analysis. The prices in a nodal system are more varied than in a zonal system. Figure 2 shows that the price spans from near zero to almost 20 $/MWh in a nodal system while the zonal system spans from about 6 to 11 $/MWh. If the zones are sensibly

defined across frequently congested interconnectors, then the prices obtained from clearing the zonal and nodal market framework are similar - exemplified in the prices in the supply excess area, where both frameworks result in stable low prices due to permanent congestion to other areas with more loads.

The social welfare obtained from the market clearing under each framework is \$1,229,906 for nodal and \$1,260,566 for zonal. The less restrictive formulation of the zonal market clearing algorithm enables a higher social welfare generation, but of course still lower than the original market clearing without any consideration of the network (which was \$1,290,958). However, the obtained social welfare from each market clearing algorithm does not translate directly to the real time network power trade as the physical limitations of the network have to be adhered to in any case. Thus, procurement of additional services will drive up the costs of the zonal market clearing compared to the nodal, which will likely result in an actual lower social welfare due to higher costs of procurement closer to real time.

Looking at the profit generation for each generator in the nodal vs. the zonal framework - table 6 - we can see that the profit is typically lower in a nodal setup where more generators will act as the marginal generators due to congestion and therefore not profit during congested periods. In a zonal setup the profit is higher as less congestion is modelled and there will be fewer marginal generators. Especially the wind farms benefit from this as their profit more than double in a zonal setup compared to a nodal setup.

Table 6: Profit for each generator in thousand \$. Generators not shown generate zero profit throughout the day.

Generator	W_1	W_2	W_3	W_4	W_5	W_6	G_6	G_7	G_8	G_9	G_{10}	G_{11}
Nodal Profit [t \$]	37.7	34.7	33.5	26.1	16.3	34.4	0	0	1.1	0	44.2	2.8
Zonal Profit [t \$]	86.0	75.7	72.2	88.0	81.8	86.6	0.6	0.6	0	5.3	43.3	1.3

5 Step 5: Balancing market

The purpose of the balancing market (BM) is to ensure the necessary up- and down-regulation is procured to ensure balance between production and consumption. The BM resembles the DA market in that it has a gate closure and is cleared. Crucially, the gate closure is very close to delivery and the market is cleared by the TSO. It follows that the BM is cleared for each hour independently, as the time of market clearing differs. In the following the BM clearing problem for hour τ is formulated:

$$\min_{\boldsymbol{p^{D,curt}},\boldsymbol{p^{G\downarrow}},\boldsymbol{p^{G\uparrow}}} \sum_{i\in\mathcal{D}} c_i^{D,curt}\boldsymbol{p^{D,curt}} + \sum_{j\in\mathcal{G}}\left[C_j^{\uparrow}\boldsymbol{p_j^{G\uparrow}} - C_j^{\downarrow}\boldsymbol{p_j^{G\downarrow}}\right] \tag{40}$$

$s.t.$

$$\boldsymbol{p^{D,curt}} + \sum_{i\in\mathcal{G}}(\boldsymbol{p_i^{G\uparrow}} - \boldsymbol{p_i^{G\downarrow}}) = \sum_{j\in\mathcal{G}_{out,\tau}} p_{j,\tau}^G + \sum_{k\in\mathcal{W}} \delta_{k,\tau} p_{k,\tau}^W \;:\; \lambda^{BM} \tag{41}$$

$$0 \le \boldsymbol{p_i^{G\uparrow}} \le \overline{P}_i^G - p_{i,\tau}^G \qquad \forall i \in \mathcal{G}\backslash\mathcal{G}_{out,\tau} \tag{42}$$

$$0 \le \boldsymbol{p_i^{G\downarrow}} \le p_{i,\tau}^G \qquad \forall i \in \mathcal{G}\backslash\mathcal{G}_{out,\tau} \tag{43}$$

$$0 \le \boldsymbol{p^{D,curt}} \le P_\tau^{total} \tag{44}$$

As evident from the objective function, the objective is to minimize the total costs of the necessary up- and down-regulation (and if needed demand curtailment). The decision variables consist of $\boldsymbol{p^{D,curt}}$, the the load curtailment, $\boldsymbol{p^{G\uparrow}}$ and $\boldsymbol{p^{G\downarrow}}$, the up and downregulation of the generators. Constraint (41) ensures that the regulation actions

(LHS) reverse the grid imbalance (RHS). Constraint (42) limits the up-regulation to the difference between the generation capacity and the DA dispatch, while constraint (43) limits the down-regulation to the DA dispatch. Finally, constraint (44) ensures that demands are not curtailed more than their DA consumption.

Now, assume the imbalance in hour $\tau = 10$ is caused by a failure for generator G_9, a 10% lower realized production of wind farms W_1 and W_2, and a 15% over-production for wind farms W_4 and W_6 compared to the DA dispatch (i.e., $\mathcal{G}_{out,10} = \{9\}$, $\delta_{1,10} = \delta_{2,10} = 0.1$, and $\delta_{4,10} = \delta_{6,10} = -0.15$). Furthermore, assume the conventional generators are the only balance providers each offering up-regulation at the DA price plus 10% of her marginal cost and down-regulation at the DA price minus 13% of her production cost (i.e., $C_j^{\uparrow} = \lambda_\tau + 0.1c_j^G$ and $C_j^{\downarrow} = \lambda_\tau - 0.13 \cdot c_j^G$). Under these conditions the BM is cleared resulting in a total regulation cost of \$4 659 and a clearing price of $\lambda^{BM} = 12.22\$/MWh$. This is higher than the DA price ($\lambda_{10}^{DA} = 10.89\$/MWh$), which indicates power deficit. Consequently, wind farms W_4 and W_6 cause positive imbalance as their realized production exceeds their DA dispatch. Thus, for these two units only, their profits in the BM differ depending on whether a one- or two-price scheme is deployed by the TSO. In the case of two-price, units causing positive imbalance are remunerated using the DA price in order to remove the incentive to plan imbalance. The other generators in two-price - and all generators in one-price - are remunerated based on the balancing price. Table 7 show the profits of each generator and wind farm using a one- and two-price scheme, respectively.

Table 7: Generator profit from day-ahead market, balancing market, and total profit during T10 under a one-price scheme. Only shown for generators participating in the balancing market.

Pricing scheme			**one-price**		**two-price**				
Unit	W_1	W_2	W_4	W_6	W_4	W_6	G_1	G_9	G_{12}
DA profits [\$]	29 835	26 712	30 754	30 137	30 754	30 137	0	38 864	0
BM profits [\$]	-177.49	-146.19	248.27	234.71	221.22	209.13	1179.42	-4 888.80	3 550.08
Total profits [\$]	29 657.23	26 565.75	31 002	30 372	30,963	30,346	1 179	33 975	3 550

6 Step 6: Reserve market

A reserve market clearing can now be implemented according to the European style where the reserve market is cleared before the day ahead market. In the reserve market only the conventional generators are expected to participate and the required up- and down-reserves are given as a percentage of the total demand in the system: $D^{\uparrow}$ and $D^{\downarrow}$. The objective is to minimize the cost of booking the reserves (eq. (45)) while meeting the reserve demand (eqs. (47) and (48)), staying within the capacity of the generators (eqs. (49) to (51)), and within the ramping constraints eqs. (52) to (55).

$$\min_{\boldsymbol{r_{i,t}^{\uparrow}}, \boldsymbol{r_{i,t}^{\downarrow}}} \sum_{t \in \mathcal{T}} \left[\sum_{i \in \mathcal{G}} r_{i,t}^{\uparrow} C_i^u + r_{i,t}^{\downarrow} C_i^d \right] \tag{45}$$

$$s.t. \tag{46}$$

$$\sum_{i \in \mathcal{G}} r_{i,t}^{\uparrow} = D^{\uparrow} \sum_{i \in \mathcal{D}} \overline{P}_i^D : \sigma^{\uparrow}, \qquad \forall t \in \mathcal{T} \tag{47}$$

$$\sum_{i \in \mathcal{G}} r_{i,t}^{\downarrow} = D^{\downarrow} \sum_{i \in \mathcal{D}} \overline{P}_i^D : \sigma^{\downarrow}, \qquad \forall t \in \mathcal{T} \tag{48}$$

$$r_{i,t}^{\uparrow} + r_{i,t}^{\downarrow} \leq \overline{P}_i^G, \qquad \forall i \in \mathcal{G}, \forall t \in \mathcal{T} \tag{49}$$
$$0 \leq r_{i,t}^{\uparrow} \leq \overline{P}_i^G, \qquad \forall i \in \mathcal{G}, \forall t \in \mathcal{T} \tag{50}$$
$$0 \leq r_{i,t}^{\downarrow} \leq \overline{P}_i^G, \qquad \forall i \in \mathcal{G}, \forall t \in \mathcal{T} \tag{51}$$
$$\underline{P}_i^R \leq \boldsymbol{r_{i,t}^{\uparrow}} - \boldsymbol{r_{i,t-1}^{\uparrow}} \leq \overline{P}_i^R, \qquad \forall i \in \mathcal{G}, \forall t \in \mathcal{T} \tag{52}$$
$$\underline{P}_i^R \leq \boldsymbol{r_{i,0}^{\uparrow}} \leq \overline{P}_i^R, \qquad \forall i \in \mathcal{G} \tag{53}$$
$$\underline{P}_i^R \leq \boldsymbol{r_{i,t}^{\downarrow}} - \boldsymbol{r_{i,t-1}^{\downarrow}} \leq \overline{P}_i^R, \qquad \forall i \in \mathcal{G}, \forall t \in \mathcal{T} \tag{54}$$
$$\underline{P}_i^R \leq \boldsymbol{r_{i,0}^{\downarrow}} \leq \overline{P}_i^R, \qquad \forall i \in \mathcal{G} \tag{55}$$

Once the reserve market is cleared the optimal values for the generators are found as $r_{i,t}^{\downarrow *}$ and $r_{i,t}^{\uparrow *}$ with market prices of $\sigma^{\downarrow *}$ and $\sigma^{\uparrow *}$ respectively. The day ahead market can then be cleared like in step 2. The only difference is that now some generators have committed to provide a reserve and they are required to participate in the day ahead market in a way that allows them to provide the regulation. The day ahead market can be cleared using eqs. (12) to (26). The only difference is that eq. (14) is substituted with eq. (56).

$$r_{i,t}^{\downarrow *} \leq p_{i,t}^G \leq \overline{P}_i^G - r_{i,t}^{\uparrow *}, \qquad \forall i \in \mathcal{G}, \forall t \in \mathcal{T} \tag{56}$$

Clearing the day ahead market conditioned on the cleared reserve market yields the day ahead prices. The up and down regulation prices can be plotted together with the day ahead price in fig. 7.

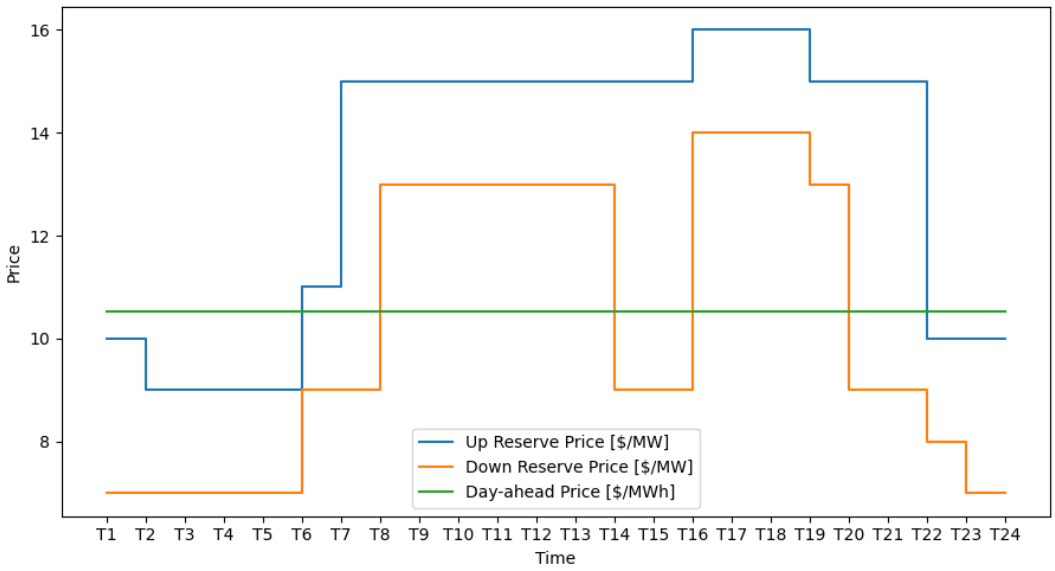

Figure 7: Up and down reserve prices together with day ahead prices.

The up regulation price is typically the highest followed by the down regulation price. The day ahead price is flat in this case at 10.52 $\$/MWh$. This has previously often been the typical price in the market as shown in table 4, only rarely rising above. Some generators has been dispatched in the reserve market that otherwise have high day ahead bids. They are forced to participate in the day ahead market but will not be the marginal generators and lose money in the day ahead market. The profit and its distribution for the active generators is shown in table 8. Here both generator 3 and 4 are loosing money due to a high participation in the reserve market, while having a high

marginal cost in a day ahead market with a low market clearing price. E.g. generator 4 has a marginal cost of 20.93 $\$/MWh$ but has to sell at 10.52 $\$/MWh$. This loss outweighs the profit made in the reserve market. The generator should reconsider its future bidding strategy in the reserve market.

Table 8: Profit of the active generator in the reserve market, day ahead market, and total profit for a 24 hour period.

Generator	G1	G2	G3	G4	G5	G8	G9	G10	W1	W2	W3	W4	W5	W6
Reserve [$]	120	120	8,540	35,820	8,820	0	0	0	0	0	0	0	0	0
Day ahead [$]	0	0	-10,002	-43,603	-1,654	43,200	48,480	75,744	33,020	29,043	27,684	33,795	31,395	33,253
Total [$]	120	120	-1,461	-7,783	7,166	43,200	48,480	75,744	33,019	29,043	27,683	33,795	31,394	33,253

References

[1] C. Ordoudis, P. Pinson, J. Morales González, and M. Zugno, *An Updated Version of the IEEE RTS 24-Bus System for Electricity Market and Power System Operation Studies.* English. Technical University of Denmark, 2016.

A Appendix

A. a) Market-clearing optimization model - KKT conditions

Lagrangian function:

$$\begin{aligned}\mathcal{L}\left(p^D, p^G, \lambda, \underline{\mu}, \overline{\mu}, \underline{\sigma}, \overline{\sigma}\right) = &- \sum_{i\in\mathcal{D}} u_i^D \, \boldsymbol{p_i^D} + \sum_{j\in\mathcal{G}} c_j^G \, \boldsymbol{p_j^G} \\ &+ \lambda \cdot \left(\sum_{i\in D} p_i^D - \sum_{j\in G} p_j^G\right) \\ &+ \sum_{i\in\mathcal{D}} \underline{\mu}_i \cdot \left(-p_i^D\right) + \sum_{i\in\mathcal{D}} \overline{\mu}_i \cdot \left(p_i^D - \overline{P}_i^D\right) \\ &+ \sum_{i\in\mathcal{G}} \underline{\sigma}_i \cdot \left(-p_i^G\right) + \sum_{i\in\mathcal{G}} \overline{\sigma}_i \cdot \left(p_i^G - \overline{P}_i^G\right)\end{aligned} \tag{57}$$

Partial derivatives:

$$\frac{\partial \mathcal{L}}{\partial p_i^D} = u_i^D + \lambda - \underline{\mu}_i + \overline{\mu}_i = 0, \qquad \forall i \in \mathcal{D} \tag{58}$$

$$\frac{\partial \mathcal{L}}{\partial p_i^G} = c_i^G - \lambda - \underline{\sigma}_i + \overline{\sigma}_i = 0, \qquad \forall i \in \mathcal{G} \tag{59}$$

Complementarity conditions:

$$\underline{\mu}_i \cdot \left(-p_i^D\right) = 0, \qquad \forall i \in \mathcal{D} \tag{60}$$

$$\overline{\mu}_i \cdot \left(p_i^D - \overline{P}_i^D\right) = 0, \qquad \forall i \in \mathcal{D} \tag{61}$$

$$\underline{\sigma}_i \cdot \left(-p_i^G\right) = 0, \qquad \forall i \in G \tag{62}$$

$$\overline{\sigma}_i \cdot \left(p_i^G - \overline{P}_i^G\right) = 0, \qquad \forall i \in \mathcal{G} \tag{63}$$

Dual constraints:

$$\underline{\mu}, \overline{\mu}, \underline{\sigma}, \overline{\sigma} \leq 0 \tag{64}$$

$$\lambda \quad \text{free} \tag{65}$$

A. b) Nodal daily prices

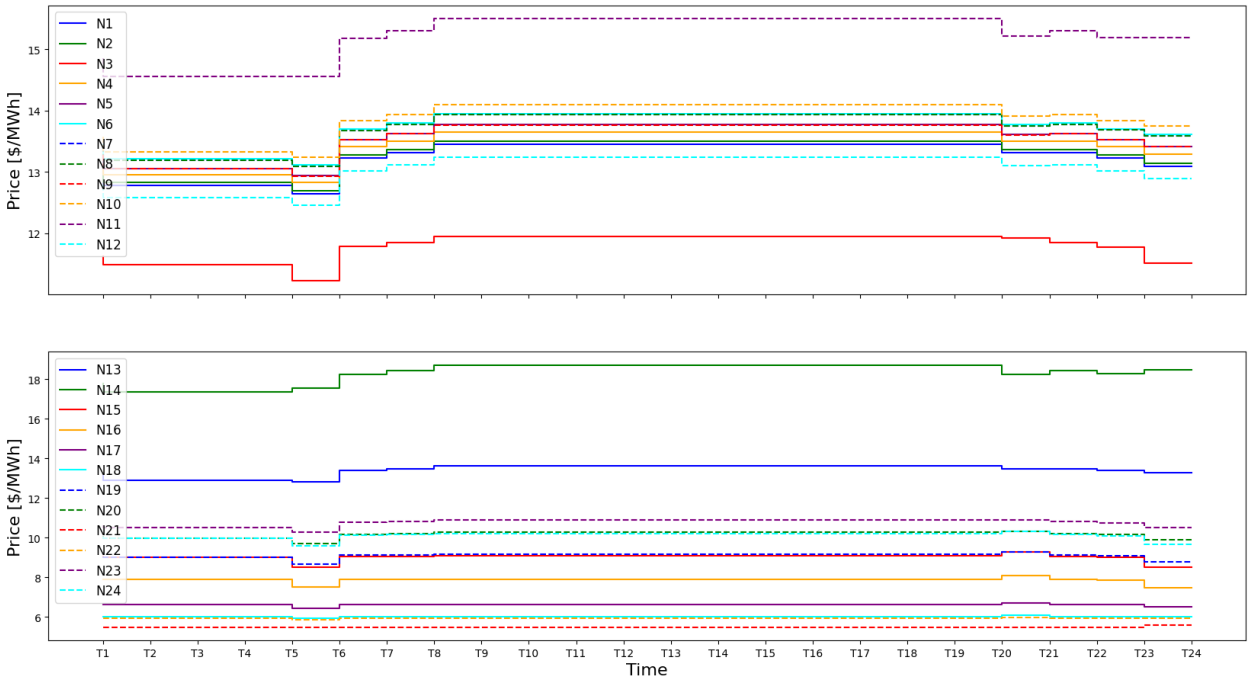

Figure 8: Price in each node during the day.

A. c) Contribution table

Group Member	Christian Witt	Frederik Fertin	Jacob Skaarup	Thomas Trosborg
Study Number	s203667	s203679	s203693	s203658
Model development	25%	25%	25%	25%
Programming	25%	25%	25%	25%
Analysis	25%	25%	25%	25%
Writing	25%	25%	25%	25%
Overall	25%	25%	25%	25%

Table 9: Contribution of each group member to the project